



JPL Document D-64582

Exoplanet Exploration Coronagraph Technology

Technology Milestone #3A White Paper (Revised)

Coronagraph Starlight Suppression Model Validation

Stuart Shaklan

May 24, 2013

**National Aeronautics and
Space Administration**

**Jet Propulsion Laboratory
California Institute of Technology
Pasadena, California**

Approvals:

Released by

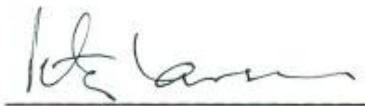


Stuart Shaklan
Principal Investigator

7-10-13

Date

Approved by



Peter Lawson
Exoplanet Exploration Program Chief Technologist, JPL

7/11/13

Date



Nicholas Siegler
Exoplanet Exploration Program Technology Manager, JPL

7/11/13

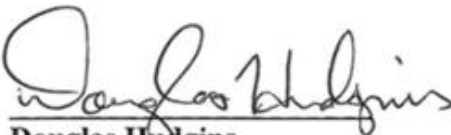
Date



Gary Blackwood
Exoplanet Exploration Program Manager, JPL

7/11/13

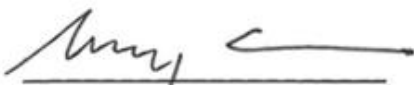
Date



Douglas Hudgins
Exoplanet Exploration Program Scientist, NASA HQ

7/17/13

Date



Anthony Garro
Exoplanet Exploration Program Executive, NASA HQ

7/22/13

Date

I. Objective

The goal of Milestone 3A (MS 3A) is to demonstrate the ability to predict the performance sensitivities of a high-contrast imaging system at levels consistent with exoplanet detection requirements. The experiments will be carried out on the High Contrast Imaging Testbed (HCIT) and the performance predictions will be made with high-fidelity optical models. The tests to be carried out will address the major items in the performance error budget, including dynamic, static, coherent, and incoherent perturbations. The tests will address image plane (occulter) and pupil plane (Lyot plane) defects in broadband (≥ 60 nm bandwidth) light. The tests described here address the physics that have been identified as playing a significant role at a contrast level of 10^{-9} . There are physical phenomena that are important at the 10^{-10} level that will be validated in future tests.

II. Introduction

a. Milestone statement

A set of 3 technology milestones for optical direct imaging was defined in 2005 [1]. Milestone 1 was the demonstration of 10^{-9} contrast imaging in monochromatic light, at a working angle of $4 \lambda/D$ (roughly the 4th Airy ring) [2]. Milestone 2 required the same contrast and working angle but over a 10% optical band [3]. The successful completions of Milestones 1 and 2 were certified by an independent review board in 2006 and 2008, respectively.

These milestones were achieved with the assistance of high-fidelity models that guided the design, implementation, and operation of the testbed. The purpose of Milestone 3 is to show the ability of the models to predict performance. Milestone 3 was originally drafted in two parts, A and B. Part A addresses model fidelity specifically for HCIT, while part B applies the models to the on-orbit prediction of a space mission. The milestone requirements are:

Milestone MS 3A: Demonstrate that starlight suppression performance predictions from high-fidelity optical models of the HCIT, utilizing measured data on specific testbed components, are consistent with actual measured results on the testbed. Correlation of model predictions with experimental testbed results validates models at a baseline contrast ratio of better than 1×10^{-9} (goal 1×10^{-10}) over a 60-nm bandwidth.

Milestone MS 3B: Demonstrate, using the modeling approach validated against the HCIT performance combined with appropriate telescope models and the current mission error budget, that TPF-C could achieve a baseline contrast of 1×10^{-10} over the required optical bandwidth necessary for detecting Earth-like planets, characterizing their properties and assessing habitability.

The focus in our MS 3A experiments is coronagraph model sensitivity validation in the HCIT testbed. Our bandpass will be from 760 – 840 nm, a 10% bandpass divided equally into five

2% bands. (While the requirement specifies a bandwidth of 60 nm, we interpret this to mean a minimum bandwidth.) These are the same filters that were used in the Milestone 2 experiments. The minimum working angle will be $4 \lambda/D$ at the central wavelength. We will use both the Milestone 2 nickel-on-glass occulting mask, as well as a second one manufactured to the same specifications. The overall layout of the testbed is similar to the Milestone 2 work with one important difference: we are using a 64 x 64 element DM stopped down to a 48 x 48 mm clear aperture. This changes the f/# of the system such that the 50% transmission point on the mask is at $3.5 \lambda/D$ at 800 nm.

This document addresses MS 3A only. Since 2007, detailed mission design has been put on hold. Thus there is not a completed mission design model on which to apply the validated optical models. In the future, for MS 3B we will employ these validated sensitivities to the representative flight system error budget to demonstrate on-orbit performance can be met.

b. Fundamental elements of dark hole contrast

The coronagraph optics and the wavefront control system are designed to create a ‘dark hole’ adjacent to the image of the star to enable observation of the feeble light of an exoplanet that will be 10^{-10} (for an Earth) and 10^{-9} (Jupiter) times fainter than the starlight. The coronagraph optics reduce diffracted light below these levels at angles greater than the Inner Working Angle (IWA). Depending on the coronagraph design, the practical limit to the inner working angle is between $2 \lambda/D$ to $4 \lambda/D$. Imperfections in the optics scatter light at all angles and become the limiting factor in the light level of the dark hole. A deformable mirror (DM) or a pair of DMs, in conjunction with an algorithm for sensing the complex electric field in the system, is used to compensate for the imperfections and creates a dark hole of sufficient contrast to observe exoplanets.

While the coronagraph can be designed to completely eliminate light from a point source over a broad band, aberrations introduce wavelength-dependent scatter that is only partially correctable across the bandpass using the DMs. Typically the wavefront control system will estimate the complex wavefront in one or several bands and the compensation algorithm will apply a weighted correction across the band. The optimal weighting function depends ultimately on the science requirements, e.g., minimize scatter across the bandpass, differentiate the planet from speckles, or perhaps minimize the scatter in a particular spectral feature.

The light level in the dark hole is often defined in terms of its “contrast.” The broadband contrast is the ratio of the average (across the bandpass) scattered starlight level in the dark hole to the average (again over the bandpass) peak light level of an unaberrated image of the star when the coronagraph mask (which blocks the starlight at the image plane) is removed.

Achieving 10^{-9} contrast in close proximity to the image of a point source requires extremely precise control of the optical system but surprisingly in a 10% bandpass it does not require exceptionally smooth and well-figured optics [4], except over a sub-mm region of the coronagraph mask itself [5]. Milestones 1 and 2 were met in HCIT using off-the-shelf off-axis ($\sim \lambda/20$) parabolas and flats. In larger bandwidths, e.g. 20%, optical quality becomes an

important limitation. In addition to optical quality, the main contributors limiting the ability to achieve high contrast are the mask design, mask imperfections, contamination, and the wavefront control system consisting of the DMs and the wavefront sensing and control algorithms. These terms comprise the core of the ‘static’ error budget which determines the ultimate contrast floor assuming a perfectly stable system. Polarization effects in the HCIT system are small compared to the 10^{-9} contrast levels expected with the faster optics and larger off-axis angles of the TPF-C design [6].

Once the wavefront has been set, maintaining 10^{-9} to 10^{-10} contrast requires sub-Angstrom aberration stability and micron-scale rigid-body motion stability of the optics, as well as high-precision stable pointing of the stellar image on the coronagraph mask. Time-dependent aberrations, rigid-body motions, and pointing errors are the main contributors to the ‘dynamic’ error budget.

These principal static and dynamic terms of the error budget will be addressed in the Milestone 3A suite of experiments.

c. **Optical models**

Milestone 3A is a test of the ability of the optical models to predict contrast and contrast sensitivity. The optical models consist of a ray-trace model, near-field diffraction codes, and a wavefront control model.

The primary coronagraph optical model is an unfolded representation of the HCIT system that performs near-field diffraction propagations through the system. It does not do ray tracing and it is not linked to an opto-mechanical-thermal finite element model. Specific attributes of the model are:

- **Point Source:** models the radial quadratic intensity variation caused by the far-field diffraction pattern of the fiber/pinhole source. This gradient is referred to as the intensity ‘droop.’ In M3A tests, we test sensitivity to the position (lateral and focus) of the source. We will not test sensitivity to the intensity droop per se, but we will test the sensitivity to beam diameter which requires an estimate of the intensity droop.
- **Optical Surfaces:** Optical surface maps are included for optics that have been measured using our Zygo instrument. Surface maps and reflectivity maps derived from representative surface Power Spectral Densities and reflectivity PSDs, respectively, are used where necessary. The surface map, typically $\lambda/20$ r.m.s. for the full optical train, is much more important than the reflectivity maps which are better than 1% r.m.s. and do not contribute to contrast at the $1e-9$ level. M3A beam walk tests will validate the sensitivity to alignment drifts for a given level of surface PSD.
- **Mask:** The occulting mask has a metallic layer and may also have a variable thickness dielectric overcoat for M3A tests. The metal coating has a thickness-dependent transmission and phase. The transmission and phase coefficients are

computed from thin film equations and the thickness is determined from the mask design and measured transmission function. Vector propagation effects are not considered. In M3A we will not test the sensitivity to mask parameters because we have already achieved agreement at better than 1×10^{-9} in broadband light in Milestone 2.

- **Deformable Mirror:** The DM is modeled as a regular array of actuators having a common influence function. A representative influence function has been measured with the surface gauge interferometer. The gain matrix in the nominal design is assumed to have the same linear response for all actuators. Hysteresis, other non-linearity, and random gain values can be added as needed for simulation purposes. In M3A we will test our sensitivity to the number of actuators and to the effects of dead actuators. We will not validate our hysteresis model – at the 10^{-9} contrast level, hysteresis affects the rate of convergence but not the level of contrast.
- **Lyot Stop:** The Lyot stop is treated as an opaque, sharp-edge mask (no vector effects are considered). It can be rotated, scaled, reshaped, etc. We will test against the effect of beam diameter (edge effects), and pupil shear, but we do not plan to directly test the positional sensitivity of the Lyot stop. This sensitivity is expected to be benign at the 10^{-9} level.
- **Wavefront Control Algorithm:** The Electric Field Conjugation (EFC) algorithm [7] will be used to control the wavefront. EFC utilizes a model of the testbed to form a sensitivity matrix that maps the actuator motion to the change in field in the image plane. It is an efficient approach with rapid convergence but its success is linked to the model accuracy. Many of the tests to be performed for Milestone 3A are tied to the algorithm's dependence on the accuracy of the optical model, e.g. what contrast is achieved if the model has the wrong mask phase function. Obviously an important aspect of wavefront control is wavefront estimation. As we have done in the past, we plan to use DM wavefront diversity to modify the electric field in the image plane and derive its complex electric field [7]. Our baseline approach is to do this in several narrow (e.g., 2%) bands, but it may also be possible to sense the wavefront in a single wide band.

In addition to the primary model, we use the JPL-developed MACOS software to determine beam-walk sensitivities through ray tracing. This program interfaces with MATLAB to generate linear sensitivity matrices for all motion degrees of freedom in the system. The beam walk is related to contrast both in a statistical sense using representative PSDs of the optical surfaces and directly using measured surface maps (and likewise for reflectivity uniformity).

We have modeled polarization and particulate contamination as well. The polarization model shows that polarization effects can be expected at about 10^{-10} contrast [8]. The particulate contamination models show on the collimating and fold optics, the larger particles, $> 20 \mu\text{m}$, play a more important role than the more numerous smaller particles [9]. Contamination levels in the testbed may be responsible for a veiling glare (incoherent scatter) which will be

uniform across the dark hole. In HCIT the narrow band veiling glare levels appears to be 2×10^{-10} . Testing of this scatter in a controlled experiment is extremely challenging and is not addressed here. We will test neither polarization nor particulate contamination models in M3A but will do so in future tests.

Detector calibration, in particular pixel-to-pixel quantum efficiency and linearity, also play a role in the performance limitations. Mainly they mildly affect the rate of convergence of the wavefront control system but this is not an issue for M3A. Since we achieved better than 10^{-9} contrast in broadband light in Milestone 2, we have seen that the detector (we will use the same one in M3A) is not a limiting factor at 10^{-9} but the effect of calibration errors grows in importance at improved contrast levels and will be the subject of future testing.

III. Coronagraph Scatter Sources

The main sources of error in high-contrast stellar coronagraphs are explained here. Depending on the coronagraph configuration, optical quality, and system stability, any of these effects can be the main factor limiting performance. The error sources are divided into coherent and incoherent, static and dynamic categories.

Coherent scatter is defined as light that responds to the wavefront estimation system. This light is not necessarily controllable in a given optical band, but it is estimable. This definition is useful for our purposes because it allows us to discriminate between scattering sources that respond to changes in the DM, and those that don't. This in turn lets us separate instrument-induced speckles from the image of a planet. For example, a 10 μm diameter particle on the occulting mask scatters starlight and creates a bright spot in the image plane that is observable (and controllable) in a sufficiently narrow bandwidth (e.g. any of the HCIT 2% bandpass filters) by reshaping the DM surface. However, there may be no DM setting that suppresses the scatter across a 10% band, resulting in a bright speckle in the broadband image. Thus the residual broadband scatter, which is not controllable, can be distinguished from a planet when analyzed in narrow bands. The scatter is coherent to our estimation system.

Incoherent scatter is light that is not observed by the estimation system; this is the total observed light minus the estimated coherent light. The light is unobservable either because the source or the light is not from the target star (the mutual coherence is zero for any practical measurement), or because the estimation system lacks spectral, spatial, temporal, or polarization resolution to observe any mutual coherence between the scatter and the estimation signal. For example, a faulty DM actuator that drifts faster than the estimation system temporal bandwidth would appear to scatter incoherent light. Scattered light that enters the detector at angles sufficient to cause sub-pixel interference would also appear to be incoherent. Incoherent scatter is sometimes referred to as a 'veiling glare' background. The wavefront control system has no effect on the incoherent scatter.

Scattering sources are considered *static* if they show no measureable change during the course of a typical astronomical observation (e.g., over 1 to 24 hrs). Examples include flaws in the mask and optical coating blemishes. The instrument design has built-in static

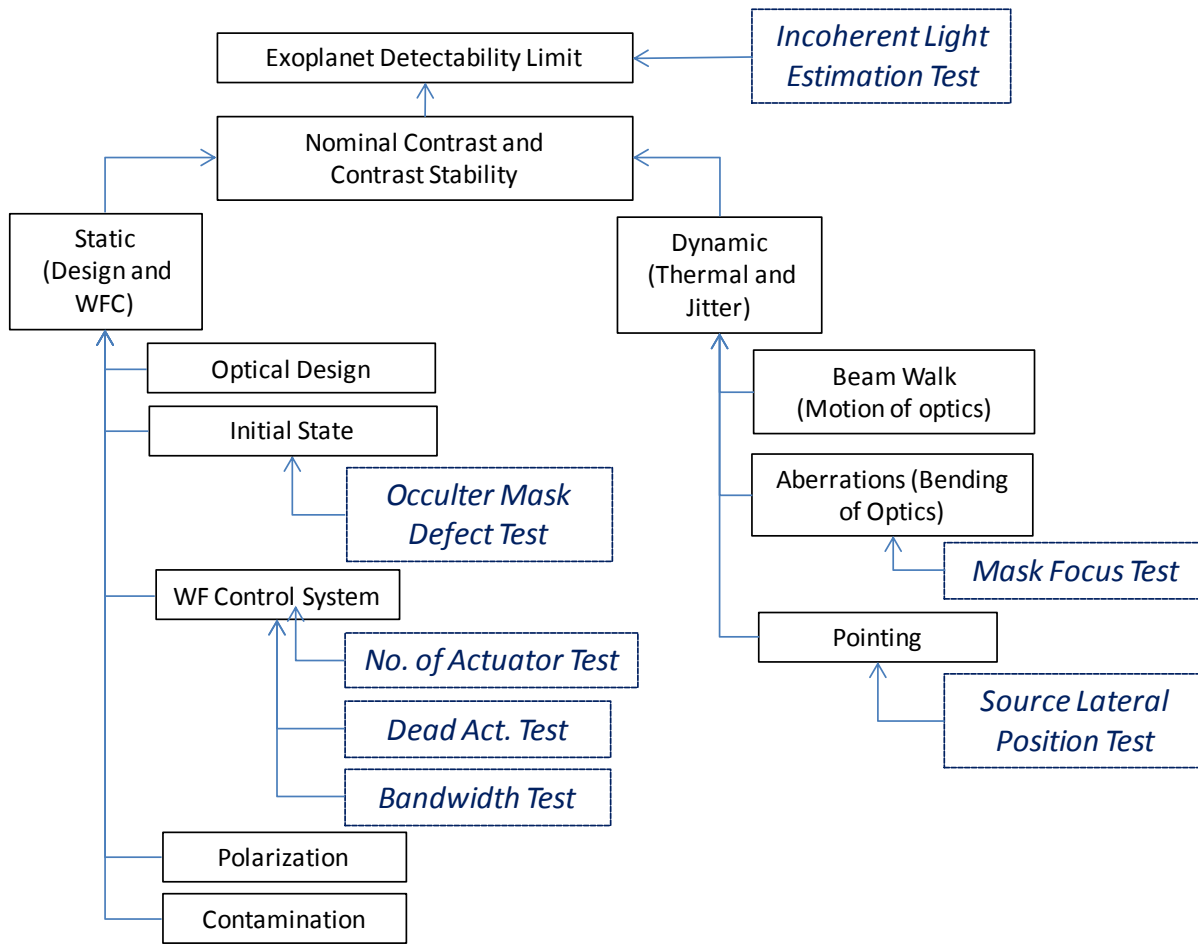


Figure 1. HCIT Error Budget structure. Black: Error terms. Blue: Milestone 3 tests.

scattering related to diffraction from edge effects (i.e. the optics are not sufficiently oversized) as well as from design trades to balance contrast across a broad optical band.

Scattering sources are called *dynamic* when they change during an observation. Dynamic errors include both thermal and vibrational effects. The main contributors are beam walk, pointing, and aberrations. Beam walk is the lateral motion of the beam across the optics resulting in misalignment (shearing) of the beam across the DM surface. The scattering wavefront is approximately given by the wavefront derivative multiplied by the shear distance. Sub-micron beam-walk can lead to significant changes in contrast. Pointing motion (e.g. the artificial point source wanders with respect to the coronagraph) contributes both beam walk and scatter due to the misalignment of the point source image on the coronagraph mask. Even when the optics are perfect, aberrations appear when the powered optics are misaligned with respect to one another and to the incident beam. Low order aberrations scatter light mainly in the middle of the image plane with diminishing energy at large working angles. They can be a limiting factor near the inner working angle.

The light level in the dark hole is a function of the scatter sources, the optical bandwidth, the optical design, and the wavefront control system. In quasi-monochromatic light, almost all

the scatter is coherent and controllable – only depolarization and the finite number of actuators limit performance. In the HCIT design, the range of incident angles across the optics is small and depolarization occurs at a contrast level well below 10^{-10} . The number of actuators in the 64x64 deformable mirror (as used, stopped down to 48x48 actuators) is also sufficient to control contrast to below 10^{-10} for the 2-10 λ/D dark hole. Thus in monochromatic light, we expect to be limited only by inadequacies in the Wavefront Control (WFC) model and by dynamic effects, but there are no fundamental physical limitations to the dark hole contrast at levels above 10^{-10} .

Broad band light presents physical limitations. The WFC system can introduce certain wavelength-dependent compensations that may not match the wavelength-dependence of the scattering sources. Also, since the WFC system operates at (or near) a pupil plane it has limited ability to perform broad-band compensation for scattering that originates in the image plane.

The error budget shown in Figure 1 provides a graphical breakdown of the various contributors to contrast degradation. This error budget is representative of the HCIT optical configuration and is expected to be applicable to flight configurations. Model validation for Milestone 3A will consist of the degree to which comparing the analytical predictions of contrast error sensitivity in the HCIT optical model agrees with experimental data collected on the HCIT testbed for various test conditions. The coronagraph model will be validated at the 10^{-9} system contrast goal achieved in Milestones 1 and 2.

The battery of tests comprising Milestone 3A addresses coherent, static, and dynamic scattering sources, in both narrow-band and broad-band light. The tests will verify that our optical models accurately represent the state of the system and that they predict sensitivities to the various scattering sources. The tests are mainly performed with a bright broadband light source, roughly equivalent to a V=-1 or -2 star. One set of tests, the alignment and focus test, uses a narrow band source. This allows us to perform the tests with minimal impact from thermal drifts in the system resulting in a more accurate measurement of the model sensitivity.

The tests are divided into two categories: open-loop and closed-loop, where open loop refers to a fixed DM setting followed by a perturbation to the system. To explore dynamic sensitivity, we perform open-loop lateral image translation and axial focus tests. These tests explore the sensitivity to contrast after the Wavefront Control System (WFCS) has been set to optimize contrast. The DM is not sent any new commands during an open-loop test. This emulates the dynamic changes to the contrast that occur during on-target integrations. We also perform a dynamic closed loop test to determine the sensitivity of the WFCS to pointing drifts during the wavefront estimation process. (Note: this test will be performed time-permitting due to its long duration.) We validate the static errors – the initial conditions when WFC is initiated –using closed-loop tests. Any deviation of the system and/or model from ideal is partially compensated by the WFCS. These tests validate our ability to specify the requirements on the quality of the occulting mask, the size and state of the DM, and the useful bandwidth.

TABLE 1

OPEN-LOOP TEST: PERTURBATION OCCURS AFTER WFCS HAS SET THE DM.

Test	Tolerancing and Sensitivity	Relevance	Experiment	Comment
Source Lateral and Focus Position	How does contrast depend on a change in the source lateral position and mask focus?	Pointing stability (tip/tilt) and focus are the most critical system parameters affecting contrast in a space telescope.	Move mask axially in at least 3 steps, and at each step, move laterally in at least 3 steps from nominal to each side.	Uses narrow band light (2% or monochromatic)

TABLE 2

CLOSED LOOP TESTS: WFCS TURNED ON DURING/AFTER PERTURBATION IS INTRODUCED

Test	Tolerancing and Sensitivity	Relevance	Experiment	Comment
Bandwidth	What is the best contrast achievable at a given bandwidth?	Tied to the number of separate starlight suppression channels used to meet science requirements.	Use increasing bandwidth (e.g., 2%, 10%, 20%) to perform wavefront control.	This will help to identify efficient means of performing wavefront control, e.g. 3 wide bands vs. 1 narrow band vs. several narrow bands.
Dead Actuators	How severe is degradation due to a dead actuator?	Important for determining manufacturing and reliability requirements.	Drive one or more actuators to their stroke limit and perform wavefront compensation using the active part of the DM. At least 3 sets of 'dead' actuators will be used	Models show that actuators that fail mid-range are tolerable. Actuators that fail at the stroke limit are difficult to compensate.
Occluder Mask Defect	What is the contrast when the occulter has an obscuring spot?	Broadband performance is highly sensitive to local defects.	Introduce an opaque spot on the mask. Measure the effect of bandpass and filter weighting on the dark hole contrast.	Dust and defects were a limiting factor in ASSIC work. Will be an important issue with circular masks. Less important for linear masks because they can be translated to 'clean' position.
Incoherent Light Estimation Accuracy	How accurate is the coherent light estimator?	Tests ability to extract incoherent signals from the data.	Perform coherent light estimation in the presence of an artificial planet signal. Subtract estimated coherent signal from image and measure SNR of planet detection	Compared phase diversity to pinhole estimation in ASSIC TDEM and found contrast agreement better than 5e-10 with nominal contrast = 4e-9.
Number of Actuators or Size of Dark Hole	How does contrast depend on the number of actuators compared to the size of the dark hole?	More elements provide more DoFs to compensate for broad band effects	Adjust dark hole size until broad band contrast control fails to converge.	Important for exo-Jupiter detections, exozodi mapping, and for digging deep around known exo-Earths.

IV. Battery of Tests

The specific set of tests to be conducted is described in Tables 1 and 2. The ‘Tolerancing and Sensitivity’ column maps directly into Figure 1. For all tests except the bandwidth and source lateral and axial position test, the experiment will operate using 10% bandwidth and the dark hole control will be a ‘D’ shape as in Milestone 2, or a rectangular shape as in the Advanced Speckle Sensing TDEM, with the working angle ranging between 4 and 10 λ/D at the central wavelength (potentially wider for the binned actuator test).

The artificial planet will be added by dividing the exposure into two parts and moving the artificial star a few λ/D to create a second point source. The first exposure is longer and is the star. The second exposure is shorter, and the source flux is reduced at the source to generate a 10^{-9} spot. The two exposures will be added to make a composite exposure that has a star and planet. For the incoherent light test, this will be done for every exposure including the probes.

V. Success Metric and Criteria

The measurement to be evaluated is: the comparison between the contrast predicted by the model and the contrast achieved in the experiment. *In each open loop test, the perturbation to be introduced shall change the model contrast from nominal by at least $s \times 10^{-9}$, where s is the step number (1, 2, 3) and shall be in agreement with the model prediction to 1×10^{-9} . In closed loop tests, the change in model contrast is evaluated after the WFCS has operated. Closed loop perturbations shall change the post-WFCS model contrast by at least 2×10^{-9} from nominal. Multiple step closed loop tests do not necessarily involve progressive delta-contrast steps.* Predicting a contrast of 3×10^{-9} to a level of 1×10^{-9} represents 33% agreement between the model and the experiment. This puts us within the factor of 2 model reserve factor that has been carried in the TPF-C error budget [10].

For open loop experiments, the model predicts a change in contrast, ΔC_p , for each step of each test. There are typically 3 steps (e.g. translate the source by 0.25, 0.5, and 0.75 microns) to each test. The experiment to be performed is to use EFC to set the contrast to a nominal value, then introduce the specified perturbation (e.g. source position motion), then remeasure the contrast without resetting the wavefront or intentionally making any further changes to the testbed. The change in contrast is evaluated as: $\Delta C_e = \text{contrast in the nominal case} - \text{contrast in the perturbed case}$. We then evaluate $M3 = \text{abs}(\Delta C_p - \Delta C_e)$. The experiment is successful if $M3 < 1 \times 10^{-9}$ contrast error for each step of each test.

For closed loop experiments, the model likewise predicts a change in contrast, ΔC_p , for each step of each test after the WFCS has operated. The experiment to be performed is to use EFC to set the contrast to a nominal value, then introduce the specified perturbation (e.g. group actuators 1x2 and then 2x2), then reemploy EFC to re-obtain good contrast. The change in contrast is evaluated as: $\Delta C_e = \text{contrast in the nominal case} - \text{contrast in the perturbed case}$. We then evaluate $M3 = \text{abs}(\Delta C_p - \Delta C_e)$. The experiment is successful if $M3 < 10^{-9}$ contrast error for each step of each test.

Since the closed loop test involves an iterative application of the wavefront control sequence, it is important to define an end point for the tests. As illustrated in Figure 2, the closed loop test will end when the best-fit rate of improvement of contrast over the current and previous 9 iterations is $\leq 2 \times 10^{-12}$ per iteration. This prevents an arbitrary stopping point if/when the change in experimental contrast comes within 10^{-9} of the model prediction.

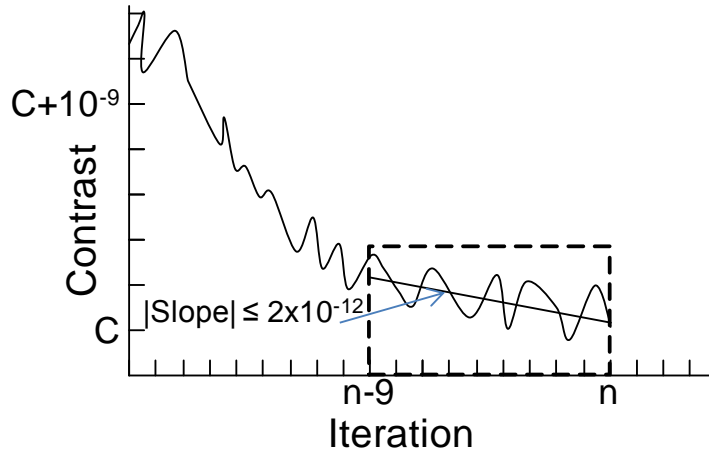


Figure 2. Slope and offset are fitted to the current and previous 9 iterations as shown. The wavefront control process is considered to have adequately converged when the magnitude of the slope is $\leq 2 \times 10^{-12}$ per iteration.

VI. Experiment Performance Goals

a. Illumination is spectrally broadband with a bandwidth $\delta \lambda \geq 60$ nm for all tests except the bandwidth-dependence test and the axial/lateral position test. The central wavelength, λ_0 , for all tests, will be in the range between 500 and 800 nm.

b. A mean contrast prediction error metric of $M3 < 1 \times 10^{-9}$ or smaller must be achieved in both an outer target dark area ranging from 4 to 10 λ_0/D and an inner area ranging from 4 to 5 λ_0/D .

Rationale: The outer area provides evidence that the high contrast field provides a useful search space for planets. The inner area tests for fundamental limitations at the inner working angle.

c. There is no minimum time or minimum number of frames required to obtain the M3A data.

d. The above tests will be repeated to produce a total of at least 3 data sets for each error source, i.e., each line in Tables 1 and 2 is performed for either three different settings (e.g. choose 3 different ‘dead’ actuators), or 3 different levels (e.g. stepping through focus and lateral translation by 100, 200, and 300 μm), or will repeat the same test 3 times. Each of the three data sets shall be obtained from experiments carried out on a separate day (e.g.

nominally 24 or more hours separation between tests). Some tests may take more than one day to complete. There is no restriction on performing separate tests (e.g. bandwidth and number of actuators) on the same day.

Rationale: *This is a test of robustness of the models and experiment repeatability.*

VII. Milestone 3A Certification Data Package

The milestone certification data package will contain the following explanations, charts, and data products, with estimates of accuracy where appropriate.

- a.** A narrative report, including a discussion of how each element of the milestone was met, an explanation of each image or group of images, appropriate tables and summary charts, and a narrative summary of the overall milestone achievement. The report shall include documentation of the speckle patterns showing how they changed with each experimental step. All test contrast data shall include error bars.
- b.** A narrative of the model and its operating assumptions and approximations.
- c.** A description of the optical elements, their significant characteristics, and their layout in the HCIT.
- d.** A tabulation of the significant operating parameters of the apparatus, including temperature stability.
- e.** An updated HCIT error budget based on measured M3A sensitivities, with appropriate documentation for each error box including a description of how error bars on model sensitivities were derived.
- f.** A calibrated image of the reference star, and an estimate of photometry errors. All contrast data shall include error bars consistent with photometric calibration and photometric noise.
- g.** Calibrated images and discussion of the occulter transmittance patterns and/or the measured transmittance profile.
- h.** Spectrum of the broadband light and an estimate of the intensity uniformity and stability of the illumination reaching the defining pupil (at the DM).
- i.** A contrast field image with appropriate numerical or color-coded or grey-scale coded contrast values indicated, and with coordinate scales indicated in units of Airy distance (λ_0/D), for each nominal starting point and perturbed image used to determine M3.

VIII. Progress Reporting

For the purpose of gauging steady progress towards Milestone #3A, the experiments outlined in Tables 1 and 2 may be reported as they are completed. These progress reports may be included in the final report for Milestone #3A but will not be subjected to formal reviews until the final Milestone #3A report is reviewed.

IX. References

1. Dooley, J., and Lawson, P., “Terrestrial Planet Finder Coronagraph (TPF-C) Technology Plan”, JPL Publication 05-8, Jet Propulsion Laboratory, March 2005 <http://planetquest.jpl.nasa.gov/TPF/TPF-CTechPlan.pdf>
2. Trauger, J., Kern, B. and Kuhnert, A., “Terrestrial Planet Finder Coronagraph (TPF-C) Milestone 1 Report - Monochromatic Contrast”, JPL D-35484, Jet Propulsion Laboratory, July 2006. http://planetquest.jpl.nasa.gov/TPF-C/TPFC_M1_Report_060710_final.pdf
3. Kern, B, Kuhnert, A. and Trauger, J., “Exoplanet Exploration Coronagraph Technology Milestone 2 Report - Broadband Contrast”, JPL D-35484, Jet Propulsion Laboratory, August 2008., <http://planetquest.jpl.nasa.gov/TPF-C/HCIT-Milestone2Signed-2008-08-08.pdf>
4. Shaklan, S. B, and Green, J. J., “Reflectivity and optical surface height requirements in a broadband coronagraph. 1. Contrast floor due to controllable spatial frequencies,” Appl. Opt., 45, 5143-5153.
5. Lay, O. P., et al, “Coronagraph mask tolerances for exo-Earth detection,” Proc. SPIE 5905 (2005).
6. Balasubramanian, K. et al, “Polarization compensating protective coatings for TPF Coronagraph optics to control contrast degrading cross polarization leakage,” Proc. SPIE 5905 (2005).
7. Give’on, A. et al., “Broadband wavefront correction algorithm for high-contrast imaging systems,” Proc. SPIE 6691 (2007).
8. Balasubramanian, K., et al., “Deep UV to NIR space telescope and exoplanet coronagraphs: a trade study on throughput, polarization, mirror coating options and requirements,” Proc. SPIE 8151 (2011).
9. Balasubramanian, K. Shaklan, S. B., and Give’on, A., “Stellar coronagraph performance impact due to particulate contamination and scatter,” Proc. SPIE 7440 (2009).
10. Shaklan, S. B., et al, “The Terrestrial Planet Finder Coronagraph Dynamics Error Budget,” Proc. SPIE 5905 (2005).

X. Appendix: Contrast Calibration Procedures

The contrast calibration procedures are identical to ones already approved and implemented for ExEP Coronagraph Milestones #1 and #2 and are repeated here for completeness.

a. Measurement of the Star Brightness

The brightness of the star is measured with the following steps.

- a.1.** The occulting mask is laterally offset, so as to place a transparent region in its transmittance profile or pattern at the location of the star image.
- a.2.** To create the photometric reference, a representative sample of short-exposure (e.g., 30 microseconds) images of the star is taken, with all coronagraph elements other than focal-plane occulters in place.
- a.3.** The images are averaged to produce a single star image. The “short-exposure peak value” of the star’s intensity is estimated. Since the star image is well-sampled in the CCD focal plane (about 20 pixels within the FWHM of the Airy disk), the star intensity can be estimated using either the value of the maximum-brightness pixel or an interpolated value representative of the apparent peak.
- a.4.** The “peak count rate” (counts/sec) is measured for exposure times of microseconds to tens of seconds.
- a.5.** The occulter transmittance profile is measured using imaging data from a microscope CCD camera. This step is used to quantify the agreement between the occulting mask specification and the occulting element on the testbed.

b. Measurement of the Coronagraph Contrast Field

Each “coronagraph contrast field” is obtained as follows:

- b.1.** The occulting mask is centered on the star image.
- b.2.** A long-exposure (typically a few seconds) image is taken of the coronagraph field (the suppressed star and surrounding speckle field). The dimensions of the target areas are defined as follows: (a) A dark field extending from $4 \lambda / D$ to $10 \lambda / D$, demonstrating a useful search space, is bounded by a straight line that passes $4 \lambda / D$ from the star at its closest point, and by a circle of radius $10 \lambda / D$ centered on the star. (b) An area within the foregoing dark field, demonstrating contrast at the inner working angle of $4 \lambda / D$, is bounded by a square box, each side measuring λ / D , such that one side is coincident with the foregoing straight line and centered on the closest point to the star.
- b.3.** The image is corrected for the attenuation pattern of the occulter and normalized to the star brightness. For this purpose, the fixed relationship between peak star brightness and the integrated light in the speckle field outside the central DM controlled area will be established, providing the basis for estimation of star brightness associated with each coronagraph image.

- b.4.** The contrast field image is averaged over the target high-contrast areas, to produce a “contrast metric.” To be explicit, the contrast metric is the sum of all contrast values, computed pixel-by-pixel in the dark field area, divided by the total number of pixels in the dark field area, without any weighting being applied. The “rms contrast” in a given area can also be calculated from the contrast field image; the average and the rms are in principle equal for an ideal monochromatic speckle field.

XI. Acknowledgements

The work described in this report was performed at the Jet Propulsion Laboratory, California Institute of Technology, under a contract with the National Aeronautics and Space Administration.

© 2013. All rights reserved.